

# Lawrence Berkeley National Laboratory

## LBL Publications

### Title

Interpretation of production tests in geothermal wells with T2Well-EWASG

### Permalink

<https://escholarship.org/uc/item/1qc2845m>

### Authors

Vasini, Ester Maria  
Battistelli, Alfredo  
Berry, Paolo  
et al.

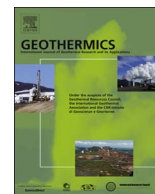
### Publication Date

2018-05-01

### DOI

10.1016/j.geothermics.2017.06.005

Peer reviewed



## Interpretation of production tests in geothermal wells with T2Well-EWASG

Ester Maria Vasini<sup>a,\*</sup>, Alfredo Battistelli<sup>b</sup>, Paolo Berry<sup>a</sup>, Stefano Bonduà<sup>a</sup>, Villiam Bortolotti<sup>a</sup>, Carlo Cormio<sup>a</sup>, Lehua Pan<sup>c</sup>

<sup>a</sup> DICAM Department, Bologna University, 40131 Bologna, Italy

<sup>b</sup> AMBEN Department, Saipem SpA, 61032 Fano, PU, Italy

<sup>c</sup> Energy Geosciences Division, Lawrence Berkeley National Laboratory, Berkeley, CA 94720, United States

### ARTICLE INFO

#### Keywords:

Coupled wellbore-reservoir flow  
Heat exchange  
TOUGH2  
T2Well  
EWASG  
Well-test interpretation

### ABSTRACT

In the geothermal sector, being able to simulate production tests by combining surface and downhole measurements can be extremely useful, improving data interpretation and reducing the impact of unavailable field data. This is possible with T2Well, a coupled wellbore-reservoir simulator. We plugged the EWASG equation of state for high enthalpy geothermal reservoirs into T2Well and extended the function to analytically compute the heat exchange between wellbore and formation at the short times. Changes to the analytical heat exchange function were verified by comparison with wellbore-formation heat exchange numerically simulated. T2Well-EWASG was validated by reproducing the flowing pressure and temperature logs taken from literature, and by using the software for the interpretation of a short production test. Simulation results indicate that T2Well-EWASG can be effectively used to improve the interpretation of production tests performed in geothermal wells.

### 1. Introduction

Numerical modelling of geothermal reservoirs is an essential tool to optimize georesource characterization and exploitation. Determining the hydraulic properties and thermodynamic conditions of a reservoir is an important aspect of the simulation process since these features are key to resource assessment and forecasting behaviour-under-exploitation scenarios. Production tests allow determination of a well's deliverability curve in terms of flow rate and enthalpy vs wellhead pressure (WHP). The flowing P & T (pressure and temperature) logs allow evaluation of feedzone location and thermodynamic characteristics. Finally, pressure transient recording, i.e. wellbore pressure changes due to controlled production or injection operations, evidence main hydrological parameters of the reservoir area drained by the well, such as: formation permeability-thickness, formation storage coefficient, skin and wellbore storage coefficients (Axelsson, 2013). Production tests duration is often limited, however, by environmental constraints such as the disposal of extracted brines, and downhole measurements are limited by safety and cost considerations such as the need for expensive tools in elevated temperature, high production wells. In this context, the possibility to reproduce via simulation the whole production test, including surface and downhole measurements, is extremely useful to improve data interpretation. In particular, coupled simulation of both wellbore and reservoir transient fluid flows allowing matching of the output production curve, flowing logs, and downhole pressure

transients, should provide a more reliable evaluation of reservoir properties. This can be done by using a coupled wellbore-reservoir numerical simulator such as T2Well (Oldenburg and Pan, 2013) and coupling it to a suitable equation of state (EOS) module for high enthalpy geothermal fluid mixtures of water, salts and non-condensable gases.

TOUGH2 (Pruess et al., 1999) is a numerical simulator for non-isothermal flows of multicomponent, multiphase fluids in one, two, and three-dimensional porous and fractured media. As well as an academic tool, TOUGH2 is also widely used for industrial applications and by government organizations (Finsterle et al., 2014).

Numerous researchers have investigated coupling TOUGH2 with a wellbore simulator. Hadgu et al. (1995) coupled TOUGH2 with the steady-state wellbore simulator WFSA used as a TOUGH2 subroutine. Bhat et al. (2005) coupled TOUGH2 with the steady-state wellbore simulator HOLA (Björnsson, 1987), designed for the modelling of single and two-phase flow of pure water in wellbores with a multi-feedzone. Tokita et al. (2005) coupled TOUGH2 with a multi-feedzone wellbore simulator called MULFEWS (Tokita and Itoi, 2004) and with a two-phase pipeline network simulator. Gudmundsdottir et al. (2012) developed a coupled wellbore-reservoir simulator using TOUGH2 and FloWell, which is a system designed to model liquid, two-phase and superheated steam steady-state flow in geothermal wells (Gudmundsdottir et al., 2012; Gudmundsdottir and Jonsson, 2015).

With the aim of accurately simulating coupled wellbore-reservoir

\* Corresponding author.

E-mail addresses: [estermaria.vasini2@unibo.it](mailto:estermaria.vasini2@unibo.it), [estermaria.vasini@gmail.com](mailto:estermaria.vasini@gmail.com) (E.M. Vasini).

flows under transient conditions, Pan and Oldenburg (2013) developed T2Well as an extension of TOUGH2. T2Well can model non-isothermal, two-phase coupled wellbore-reservoir flow for generic multi-component mixtures by using a suitable EOS module.

In this study, the T2Well wellbore-reservoir numerical simulator was coupled to the EWASG EOS module developed for high enthalpy geothermal reservoirs containing 3-component mixtures of water, NaCl and a non-condensable gas (NCG) (Battistelli et al., 1997; Battistelli, 2012). In addition, improvements were made to the analytical computation of heat exchange between the well and the surrounding formations at the short times. T2Well-EWASG was verified by comparing the results of the modified analytical wellbore-formation heat exchange function with wellbore-formation heat exchange numerically simulated. T2Well-EWASG was validated by reproducing two published flowing P & T logs recorded in wells producing brine with remarkable amounts of CO<sub>2</sub> and a short production test, the latter performed in a recently drilled exploration well in the Wotten Waven field, Commonwealth of Dominica. All the experimental data are related to reservoir containing NaCl and CO<sub>2</sub>. The new T2Well-EWASG can be used for the interpretation of well tests by combining surface and downhole measurements and to simulate the exploitation of high enthalpy geothermal systems.

## 2. T2Well

T2Well extends the existing numerical reservoir simulator TOUGH2 by introducing a special wellbore sub-domain in the numerical grid. Wellbore flow is simulated by solving the one-dimensional momentum equation. In the case of two-phase wellbore flow, the Drift Flux Model (Shi et al., 2005; Zuber and Findlay, 1965) combines two momentum equations of two phases to create a single momentum equation of the mixture. Like TOUGH2, T2Well can be used with different EOS to describe different fluid mixtures. Thus far, T2Well has been used with ECO2N (Pruess, 2005) for applications related to CO<sub>2</sub> sequestration, with ECO2H (Pan et al., 2011, 2015) for enhanced geothermal system simulations, with EOS7C (Oldenburg and Pan, 2013) for applications related to compressed air energy storage, and with EOIL to model Macondo well blowout (Oldenburg et al., 2011). The heat exchanges between wellbore and the surrounding formation can be numerically simulated, or optionally calculated with Ramey's analytical method (Ramey, 1962) or Zhang's convolution method (Zhang et al., 2011). Details of T2Well characteristics and numerical formulation can be found in Pan and Oldenburg (2013).

## 3. EWASG EOS module

EWASG (Equation-of-state for WAter, Salt and Gas) is a TOUGH2 EOS module developed primarily to model hydrothermal systems containing dissolved solids and one non-condensable gas (NCG) such as CO<sub>2</sub>, CH<sub>4</sub>, H<sub>2</sub>S, H<sub>2</sub> or N<sub>2</sub> (Battistelli et al., 1997). EWASG can handle phase equilibria and fluid property calculations up to 350 °C and 100 MPa for H<sub>2</sub>O-NaCl-NCG mixtures found in low and high enthalpy geothermal reservoirs, with the limitation of low to moderate NCG partial pressures. Compared to the version included in TOUGH2V.2.0 (Pruess et al., 1999), the EWASG version, jointed to T2Well, implements several major improvements (Battistelli et al., 2012), namely:

- IAPWS-IF97 correlations for pure water and steam (IAPWS, 1997; Croucher and O'Sullivan, 2008) and a more recent formulation for water and steam viscosity (IAPWS, 2008).
- An internally consistent H<sub>2</sub>O-NaCl EOS package derived from the work of Driesner and Heinrich (2007) and Driesner (2007) to effectively covering the entire P-T-X area of interest (T = 0-350 °C; P = 0-100 MPa; NaCl mass fraction = 0-1);
- A more consistent approach to vapour pressure lowering (VPL) and water adsorption, including the dependency of capillary pressure on

temperature and salt concentration.

- Enhanced, albeit still simplified, modelling of NaCl partitioning in the gas phase to improve transitions phase from two-phase to single gas phase and vice versa.

EWASG has subsequently been coupled with other simulators belonging to the TOUGH2 family of codes (Battistelli, 2012), such as iTOUGH2 (Finsterle, 2007) and TOUGH-MP (Zhang et al., 2008). EWASG was also used as the starting point for the development of new TOUGH2 EOS modules such as ECO2 and ECO2N. Its correlations for brine properties have been included in other TOUGH2 EOS modules such as EOSM, TMVOC V.2.0 (Battistelli, 2008) and TMGAS (Battistelli and Marcolini, 2009).

## 4. Modification of the analytical calculation of heat exchange between wellbore and formation

The availability of analytical computational methods to calculate wellbore-formation heat exchange allows substantial simplification of grid discretization, thereby reducing both the complexity of the numerical model and computational time. However, both methods implemented in the original version of T2Well have some limitations. Ramey's (1962) method works effectively only for times longer than approximately a week, and so is not suitable for the study of short transient phenomena. Zhang's et al. (2011) method, on the other hand, uses a simplified wellbore design, assuming there is no thermal resistance related to well completion. To overcome these limitations, the Ramey analytical function for heat exchange between wellbore and formation was modified by introducing the Chiu and Thakur (1991) time function. As suggested by Ramey (1962), thermal resistance of the wellbore completion was also taken into account with the introduction of this author's expression for wellbore heat conduction rate:

$$dq = \frac{2\pi r_1 U (T_1 - T_E)}{r_1 U f(t_D) + k_T} dz \quad (1)$$

Where:  $r_1$  is the wellbore radius (m),  $f(t_D)$  the time function,  $t_D = \frac{\alpha t}{r_1^2}$  the dimensionless time,  $\alpha = \frac{k_T}{\rho c}$ ,  $c$  the specific heat,  $\rho$  the density of the formation and  $r_2$  the well completion radius,  $T_1$  the wellbore temperature,  $T_E$  the formation temperature,  $k_T$  the thermal conductivity of the formation,  $dz$  differential element of depth, and  $U$  the over-all heat transfer coefficient of well completion as defined by Willhite (1967).

Moreover, the following time function by Chiu and Thakur (1991) was added to T2Well:

$$f(t_D) = 0.982 \ln(1 + 1.81t_D) \quad (2)$$

which is in good agreement with the exact solution of Carslaw and Jaeger (1959) for all the times, as shown in Fig. 1.

Willhite (1967) provides the general expression for computation of the overall heat transfer coefficient ( $U$ ) which is carried out considering wellbore completion as a series of thermal resistors for radial heat transfer. Starting from the Willhite's expression, and assuming that the inner casing wall is in thermal equilibrium with the flowing fluid and that the casing resistors are negligible, in the case of a single cemented annulus the fluid produced flows in the production casing and  $U$  is given by:

$$U = \frac{k_{cem}}{r_1 \ln \frac{r_2}{r_1}} \quad (3)$$

where  $r_1$  is the wellbore radius,  $r_2$  the completion radius and  $k_{cem}$  the thermal conductivity of the wellbore completion.

## 5. Verification and validation of T2Well-EWASG

The modifications made to T2Well-EWASG, were tested to verify the new analytical equation for the heat flux with and without the wellbore

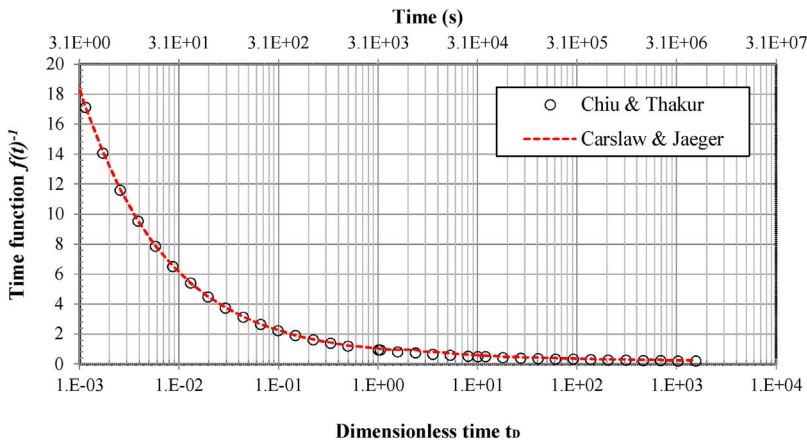


Fig. 1. Comparison of Chiu and Thakur time function with the Carslaw and Jaeger exact solution.

completion effect.

Validation of these changes consisted in reproducing the flowing pressure and temperature profiles reported in the literature and in interpreting field production tests with a full-coupled wellbore-reservoir simulation.

### 5.1. Verification of the analytical heat exchange option

Example 1 of the Zhang et al.’s paper (2011), was used to verify the analytical computation of wellbore-formation heat exchange. We considered a 1 m section of a wellbore with a radius of 0.05 m initially full of water at 100 °C. The temperature of the fluid inside the wellbore was kept constant. The rock formation around the wellbore had a fixed initial temperature of 20 °C, density 2600 kg m<sup>-3</sup>, heat conductivity of 2.1 W °C<sup>-1</sup> m<sup>-1</sup> and a specific heat of 1000 J °C<sup>-1</sup> kg<sup>-1</sup>. For the simulation using the analytical option, the numerical grid was limited to the wellbore only (at least two well blocks are required by T2Well). For the heat exchange numerically simulated, the grid included the wellbore and the surrounding formation discretized with 185 radial elements. The radius of the radial grid is incremented by 5%, moving from the wellbore to the outer radial boundary, which was set at about 400 m from the well axis. The initial temperature at the radial lateral boundary was kept constant during the simulation. A negligible permeability (10<sup>-20</sup> m<sup>2</sup>) was assigned to the rock formation so as to avoid fluid mass fluxes. The results of the using the analytic function were found to be in good agreement with the those numerically simulated, as shown in Fig. 2 (curves labeled “without completion”), where heat flux values between wellbore and formation as a function of time is plotted. Again, the analytical results obtained when wellbore completion was taken into account were compared with the heat exchange numerically simulated (Fig. 2, curves labeled “with completion”). In this case, the numerical grid consists of the wellbore (r = 0.05 m), surrounded by a

radial element representing the completion (r = 0.10 m). The radius of the radial grid was incremented by 5%, moving from the wellbore completion to an outer radial boundary set at about 450 m, where constant temperature conditions of 20 °C were maintained during the simulation. The thermal conductivity of the completion (cement) was set at 1.4 W °C<sup>-1</sup> m<sup>-1</sup>, while negligible density, porosity and specific heat were assigned in accordance with the assumption made by Ramey (1962), as shown in Eq. (1). When the analytical function is used, two additional parameters are requested in the simulation input file: the completion radius and the overall heat transfer coefficient (in our case U = 40.395 W °C<sup>-1</sup> m<sup>-1</sup>) computed with Eq. (3). A comparison of the heat flux between the wellbore and the formation, as illustrated in Fig. 2, shows that, apart from the first 100 s, agreement between the two results is good.

Comparison between the results obtained when wellbore completion, was taken into account or not, evidences the effect exerted by well completion, which in this case proved to be considerable at the short times.

When the analytical function is used, to model the temperature transients driven by the conductive heat flow in the upper-cased section of the well, the grid around the well is not necessary. This simplify the grid construction and speeding up the simulation. On the other hand, since Eq. (1) derived by Ramey (1962) assumes constant wellbore temperature, it provides reliable results when well production, or re-injection, is performed at fairly constant conditions, like those found in long term production or injection operations. When considering at short transients driven by rate changes, a more rigorous use of eq. 1 would require the application of the superposition principle as discussed by Chiu and Thakur (1991) and Zhang et al. (2011). It should be remembered that the calculated heat loss must subsequently divided by the flowing mass rate to evaluate the effect on fluid enthalpy. As the mass flow in producing geothermal wells is significant, a non-accurate

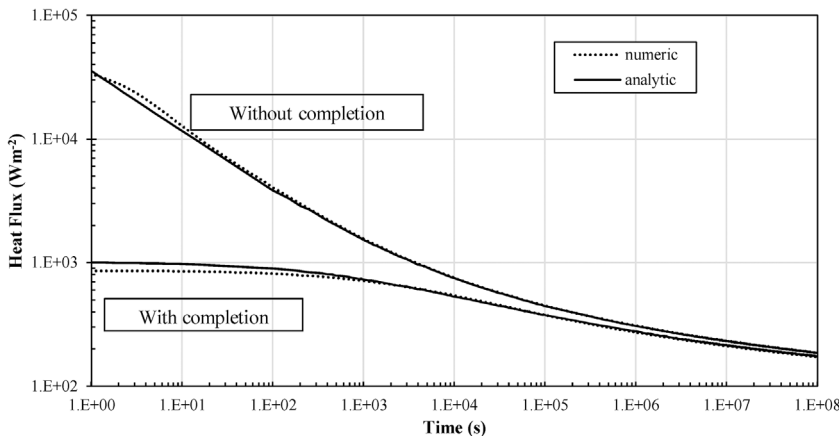


Fig. 2. Heat flux between the wellbore cell and the formation vs time with and without the well completion, comparison between the numerical and analytical results.

evaluation of heat transfer vs time usually has a limited effect on fluid enthalpy and flowing temperatures.

### 5.2. Validation of wellbore flow in geothermal wells

Validation of T2Well-EWASG’s capability to model the wellbore flow in geothermal wells was performed by reproducing published flowing temperature and pressure logs recorded in geothermal wells producing brine with dissolved CO<sub>2</sub>. Two flowing logs were chosen from the literature: the first referred to well W2 (Barelli et al., 1982), the second to well KD13 (James, 1975). Since initial wellbore pressure and temperature conditions were not given in either case, we assigned reasonable initial conditions to reproduce the measured logs on the assumption that these were recorded when the wellbore flow was close to the steady-state. The T2Well was used to simulate the well opening and subsequent discharge, until reaching almost steady-state conditions. The transient behaviour was simulated by assigning constant bottom-hole pressure, temperature and composition conditions, and a set of geothermal fluid extraction rate from the wellhead element. The discharge rate was gradually increased at the beginning to mimic well opening and to avoid steps of excessively short duration. The rate was then held constant at the value reported in the literature.

Well W2 is 1355 m deep and produces low salinity brine (9600 ppm of mass fraction) with large amounts of CO<sub>2</sub> (20,000-100,000 ppm of mass fraction). It is completed with a 13 3/8” (0.334 m) production casing. The measured flowing bottom temperature was 225 °C while pressure was 9.8 MPa. A linear temperature profile was assigned with a bottom temperature of 225 °C and a wellhead temperature of 35 °C. The initial pressure profile was hydrostatic from the bottom (pressure 9.8 MPa) to 400 m, while from 400 m to the wellhead, it was assumed to be gas static. Fig. 3(a) shows the temperature and pressure profiles used as initial conditions. The well mesh has 47 elements, representing only the wellbore, with constant conditions set at the bottom including CO<sub>2</sub> and NaCl mass fraction contents of 30000 ppm and 9600 ppm, respectively, as reported by Barelli et al., 1982.

Well KD13 is 700 m deep and completed with a 9 5/8” (0.222 m) production casing. It produces a low salinity brine with a salt mass fraction of 1000 ppm and a large CO<sub>2</sub> concentration (mass fraction equal to 20000 ppm). Bottom flowing temperature and pressure were 193 °C and 5.5 MPa, respectively. A linear temperature profile was assigned with a bottom temperature of 200 °C and a wellhead temperature of 100 °C. The initial pressure profile was assumed to be hydrostatic from the bottom up to 150 m, and from that point upwards to be

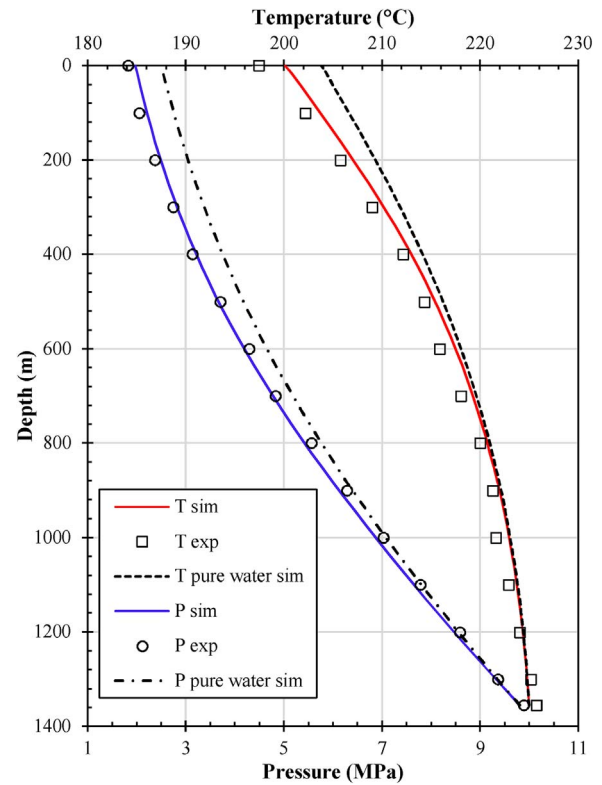


Fig. 4. Comparison between experimental data and simulation results for the flowing temperature and pressure profiles of well W2 after 11 h of production.

gas static. Initial temperature and pressure profiles are shown in Fig. 3(b). The wellbore was discretized with 15 elements and the heat exchange is simulated with the analytical function.

Fig. 4 compares the simulated flowing P & T profiles of well W2 after 11 h of production at 34.1 kg s<sup>-1</sup> (considering the two cases, pure water, and water with salt and CO<sub>2</sub>) with the experimental data. Taking the chemistry of the reservoir fluids into account, the match between the experimental data and the simulated results when water with salt and CO<sub>2</sub> is considered, is reasonably good. The maximum absolute difference between the simulated and experimental temperature values is 1.17%, while the average value is 0.61%. The average percentage difference between simulated and experimental pressure readings is

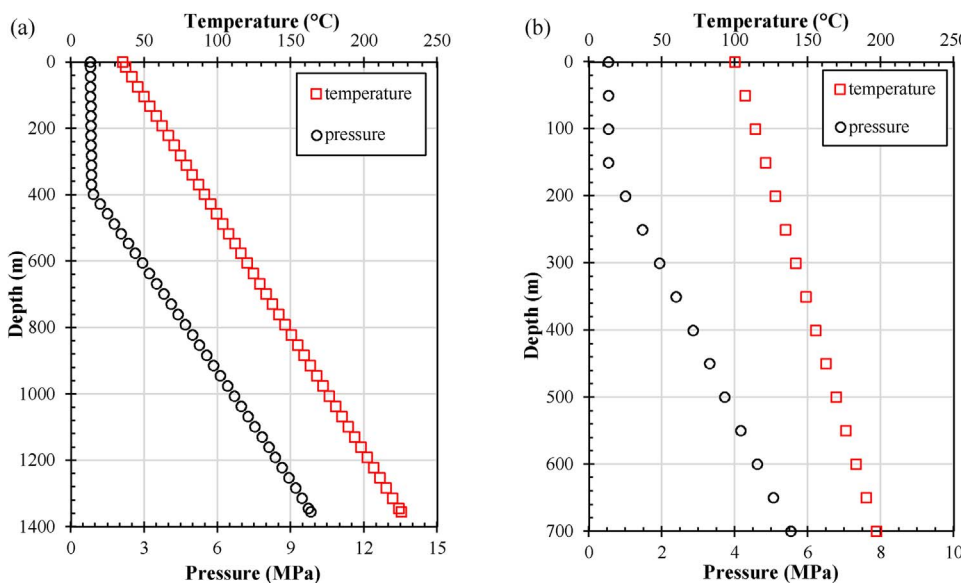


Fig. 3. Pressure and temperature profiles used as initial conditions for the simulation of wells W2 (a) and KD13 (b).

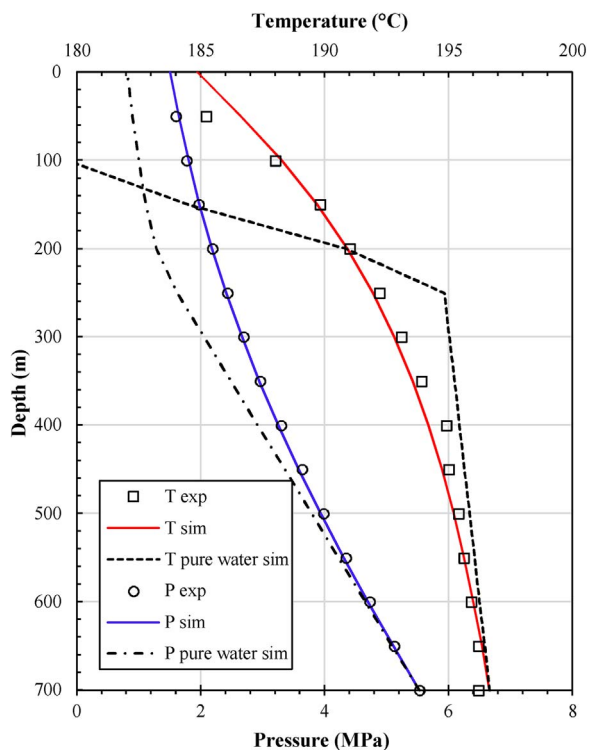


Fig. 5. Comparison between experimental data and simulation results for the flowing temperature and pressure profiles of well KD13 after 100 h of production.

2.8%.

Fig. 5 shows the simulated flowing temperature and pressure profiles of well KD13 after 100 h at a production rate of  $90.56 \text{ kg s}^{-1}$  (also considering the case with pure water). In the case of water with salt and  $\text{CO}_2$ , the agreement with the experimental data is good. The difference between experimental and simulated results is 0.17% for temperature and 0.91% for pressure. The same simulations, for both wellbores W2 and KD13, performed without salt and  $\text{CO}_2$  do not show a similar agreement between the simulated and experimental data. In this case, the high  $\text{CO}_2$  and salt content cannot be ignored, with the result that a proper equation of state has to be chosen. This highlights the usefulness of the thermodynamic description of EWASG. The above results show that T2Well-EWASG can simulate wellbore flow at conditions found in geothermal wells discharging two-phase  $\text{H}_2\text{O-CO}_2\text{-NaCl}$  mixtures. Future work will include checking the code with respect to a wider range of PTX conditions.

### 5.3. Validation with respect to coupled wellbore-reservoir flow in geothermal fields

To validate T2Well-EWASG's capability of simulating coupled wellbore-reservoir flow in geothermal systems, a fully-coupled wellbore-reservoir simulation was performed. Field data were collected during the short production test performed on well WW-01, (ELC Electroconsult, 2013; Osborn et al., 2014). WW-01 is a slim vertical 1200 m hole producing from a liquid-dominated reservoir in a volcanic environment. The reservoir brine has an estimated NaCl and  $\text{CO}_2$  mass fraction content of 6000 ppm and 1760 ppm, respectively. Maximum temperature and pressure of 238 °C and 10.2 MPa, respectively, were measured under shut-in conditions. The conceptual model is shown in Fig. 6. The WW-01 well-reservoir model included the cap-rock from 0 to -297 m, and three main feed zones: the first located between -297 m and -344 m (FEED1), the second between -710 m and -734 m (FEED2) and the third between -880 m and -940 m (FEED3). The model also had reservoir layers called RESV1 and RESV2 between the feedzones, and a less permeable rock domain (BOTTM) beneath the

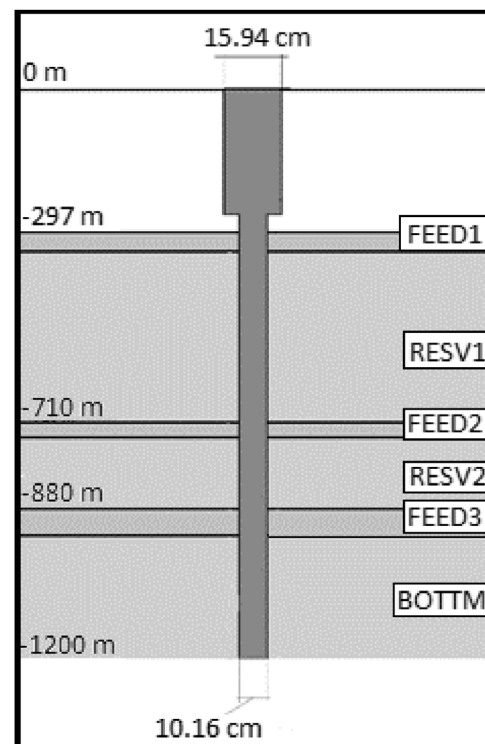


Fig. 6. Conceptual model: well WW-1 and formation.

third feedzone. The well was completed with a 7" production casing with an internal diameter of 0.159 m and a 4 ½" slotted liner of 0.102 m internal diameter. The liner hanger was set at -263 m. The 2D radial grid used for the wellbore-reservoir system extended to an outer radius of 1500 m with the wellbore located on the axis of symmetry, for a total of 1658 elements.

Fig. 7 illustrates the vertical cross section of the model, obtained with TOUGH2Viewer (Bonduá et al., 2012), in which the main feed-zones (in lighter colour) and the change in wellbore diameter can be seen. Note that TOUGH2Viewer visualizes 2D radial symmetric grid elements as hexahedral blocks. The cap-rock has not been included in the model in terms of grid blocks. In this case, the heat exchange between wellbore and cap-rock above 297 m depth was simulated using the original T2Well analytical function.

Fig. 8 shows the WW-01 shut-in temperature and pressure logs measured during well warm-up subsequent to the drilling operations and completion tests. They are believed to be sufficiently close to reservoir conditions and were therefore adopted as tentative initial conditions for the steady state simulation. In fact, as shown in Fig. 8, the formation temperature assumed for production at FEED2 and FEED3 was slightly modified, and used as a matching parameter enabling better reproduction of a recorded flowing temperature log.

This probably implies that the shut-in temperature log was not yet stabilized after the disturbances caused by drilling operations and completion tests. This is indeed a frequently observed phenomenon when field operations are speeded up in order to acquire preliminary field data required for fast decision making. Recorded data are displayed in Fig. 9 on a pressure-temperature plot with the pure water saturation curve. The plot is useful to identify the flash conditions (238 °C and 3.53 MPa g - relative pressure -) and to estimate the NCG partial pressure (0.4 MPa). The inflows at FEED2 and FEED3 are clearly identified.

The wellbore's production history, (Table 1) was assigned to the model using a time-dependent fluid extraction from the top element of the wellbore grid. The field test was performed using a horizontal line with a lip pressure pipe discharging into an atmospheric separator

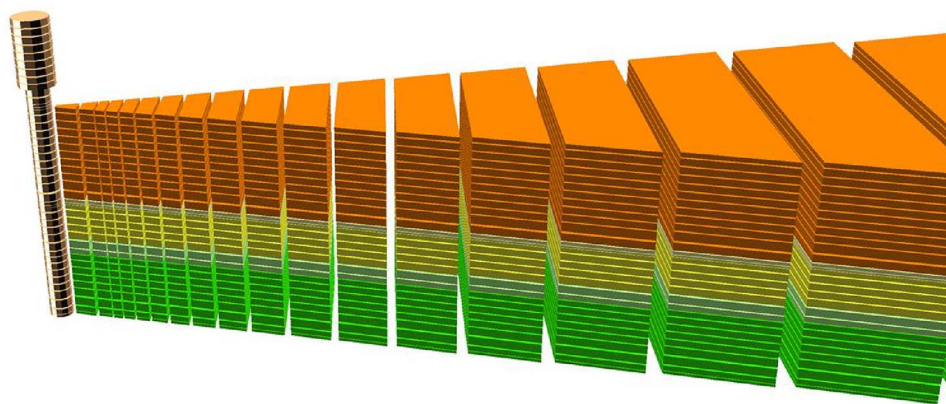


Fig. 7. 2D vertical section of WW-01 wellbore-reservoir model. The main feedzones are indicated in lighter colours. Visualization of the model was performed by TOUGH2Viewer (Bonduá et al., 2015). To visualize the well, vertical exaggeration was set at 0.001 times.

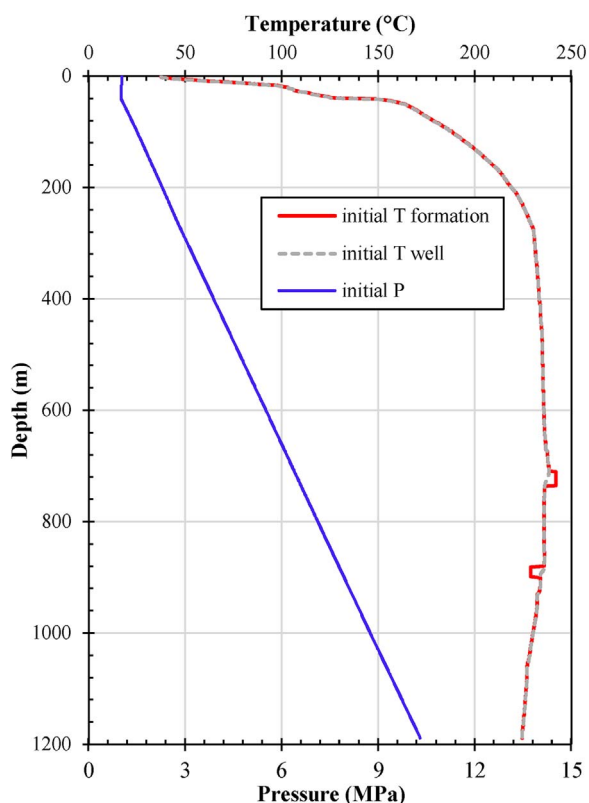


Fig. 8. Initial pressure and temperature conditions assumed for the wellbore-reservoir model.

equipped with a weir box. Total mass and mixture enthalpy were computed using the James (1962) equation for the critical flow at the lip pipe combined with the isenthalpic flash at atmospheric conditions.

The history-matching process involves reproducing the experimental data by simulating the production history. In this first application of T2Well-EWASG to the WW-01 test data, the possible contribution of FEED1 was ignored, and it was assumed that only FEED2 and FEED3 were producing. As shown in Fig. 10 production history was assumed, to have a stepped progression, each step corresponding to available field measurements.

The experimental data considered consist of two downhole pressure transients, one flowing pressure and temperature log, the WHP and lip pressure measurements, and the brine level measurements at the weir box. Surface measurements were used to compute total mass rate and discharge enthalpy at wellhead conditions. Downhole pressure was continuously recorded at depths of 800 m and 1180 m during the two pressure transient tests. The permeability of different rock domains was varied in order to reproduce the experimental results. Table 2

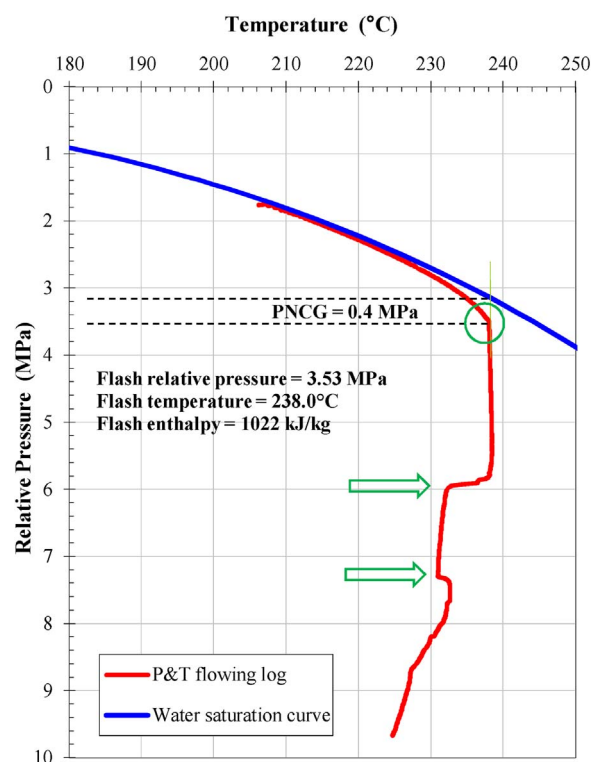


Fig. 9. Measured P & T log data plotted with the pure water saturation curve, with estimated flash conditions and partial pressure of NCG.

summarizes the horizontal permeability values obtained by calibration of the model. For this preliminary study, we assumed that the skin coefficient of the wellbore was zero.

Figs. 11 and 12 show a reasonably good match of the measured flowing pressure and temperature profiles with the simulated data. The percentage difference for the temperature values is 0.37%, and 2.12% for the pressure. Both simulated P & T overestimate measured values in the upper 300 m above the location of inferred FEED1, which was not considered in these preliminary simulations.

Fig. 13 shows pressures recorded at 800 m, 1180 m depth and at wellhead and the simulated results. The agreement between recorded and simulated pressure is reasonably good up to 21000 s, while the WHP and downhole pressures are underestimated after 21000 s.

Fig. 14 shows the comparison between production enthalpy computed using field data and the numerical simulation results. The simulated results give an almost constant production specific enthalpy of about 1011 kJ kg<sup>-1</sup>: considering the potential energy loss between the ground surface and a flash depth at slightly above 400 m, flash enthalpy is about 1015 kJ kg<sup>-1</sup>, slightly lower than the 1022 kJ kg<sup>-1</sup> estimated

**Table 1**  
Production history of wellbore WW-01.

Time	Total flow (kg s <sup>-1</sup> )	WHP (MPa)	Enthalpy (kJ kg <sup>-1</sup> )	Remarks
08:55		0.45		
09:00		0.45		well opening
09:05	31.3	1.80	1088	
09:14	26.9	1.80	1125	
09:25	26.3	1.78	1237	
09:45	25.6	1.78	1280	
10:00	24.5	1.79	1223	opening
10:15	22.7	1.79	1170	
10:30	27.3	1.75	1290	
11:18	25.0	1.75	1332	
11:40	27.3	1.75	1230	
12:25	25.0	1.75	1292	
12:45	28.7	1.75	1163	
12:50				throttling
12:55	26.0	1.79	1223	
13:15	27.1	1.79	1178	
13:50	28.6	1.78	1156	
14:15	27.1	1.77	1155	
14:40				throttling
14:45	16.8	19.4	1148	
14:55	17.3	2.02	1095	
15:05	16.4	2.02	1169	
15:25	16.3	2.02	1157	
15:45	17.2	2.03	1105	
15:57				throttling
16:02	8.3	2.08	1156	
16:15	8.0	2.08	1184	
16:30	8.0	2.08	1184	
16:50	0.0	2.08		well shut-in
18:00	0.0			pool out of hole

for the brine at flash conditions. The enthalpy change due to heat transfer is quite limited because the initial formation temperature is quite close to the flowing temperature. Although an almost constant wellhead enthalpy is in agreement with production from a liquid dominated geothermal reservoir, the simulated values underestimate the data derived from field measurements as shown in Fig. 14 of about 250 kJ kg<sup>-1</sup> in the first period up to 15000 s, and of about 140 kJ kg<sup>-1</sup> in the second period. The reduction of measured enthalpy is not exactly correlated with the reduction of discharge rate which takes effect after 20700 s.

The higher enthalpy given by the field data has already been evidenced in the ELC Electroconsult (2013) report. This fairly short-

**Table 2**  
Reservoir formation permeability (horizontal) as obtained by model calibration.

Rock type	Horiz. permeability (m <sup>2</sup> )
FEED1	15.0 × 10 <sup>-15</sup>
RESV1	1.5 × 10 <sup>-15</sup>
FEED2	150.0 × 10 <sup>-15</sup>
RESV2	0.5 × 10 <sup>-15</sup>
FEED3	30.0 × 10 <sup>-15</sup>
BOTTM	0.02 × 10 <sup>-15</sup>

duration production test, performed using the Russell James method with a lip pipe discharging into an atmospheric pressure separator, measured the separated brine flow with a V-shaped weir. The higher estimated enthalpy result could be due to:

- Measurement errors during the production tests and/or;
- The contribution of the first feedzone not considered in the present model.

In this preliminary study, we adjusted only the horizontal permeability of FEED2 and FEED3 in order to match the field data but did not attempt to simulate the behaviour of all the feed zones in greater detail. For this reason, the second point mentioned will be the object of further study since the first feed zone below the cap-rock is in two-phase conditions. FEED1 could then increase production enthalpy by discharging a two-phase mixture with excess steam with respect to the static feed temperature. By discharging pure steam at local conditions (232 °C), FEED1 should contribute to 5, 10 and 15% of the total discharge rate and increase the mixture enthalpy to about 1112, 1200 and 1290 kJ kg<sup>-1</sup>, respectively. This significant contribution should then be verified by simulating its effects on measured P & T logs, since the present model is slightly overestimates recorded flowing P & T in the upper 300 m.

On the other hand, possible measurement errors might derive from:

- Unreported instrumentation problems;
- Reduced separator efficiency, as liquid water was discharged at the separator top (carryover), with an underestimation of liquid rate and an overestimation of mixture enthalpy. To obtain the enthalpy inferred from the flash temperature, the brine carried over the silencer should be in the order of 30% of that measured at the weir box, which seems highly unlikely. The carryover was enhanced by

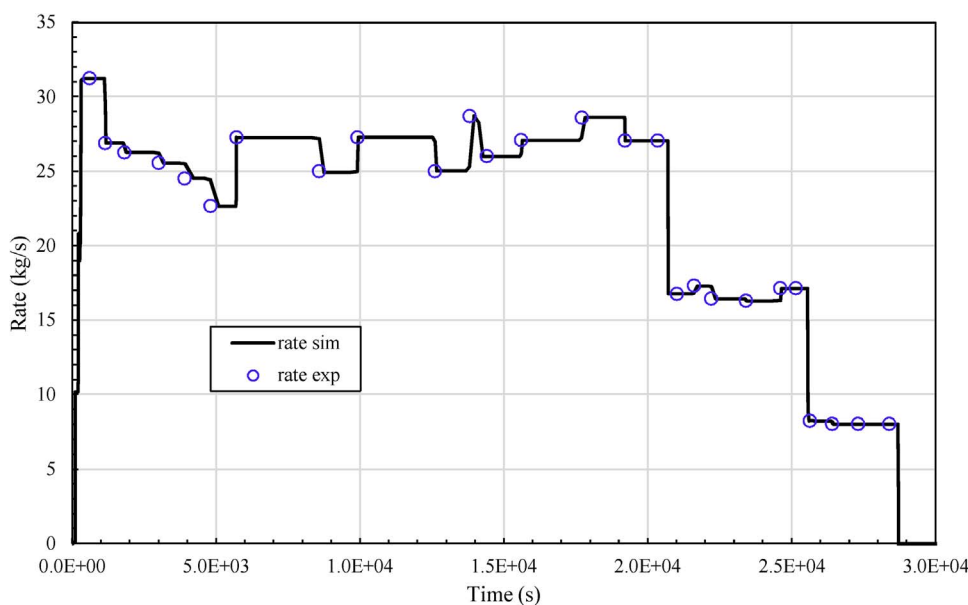


**Fig. 10.** Comparison between simulated and measured discharge rate.



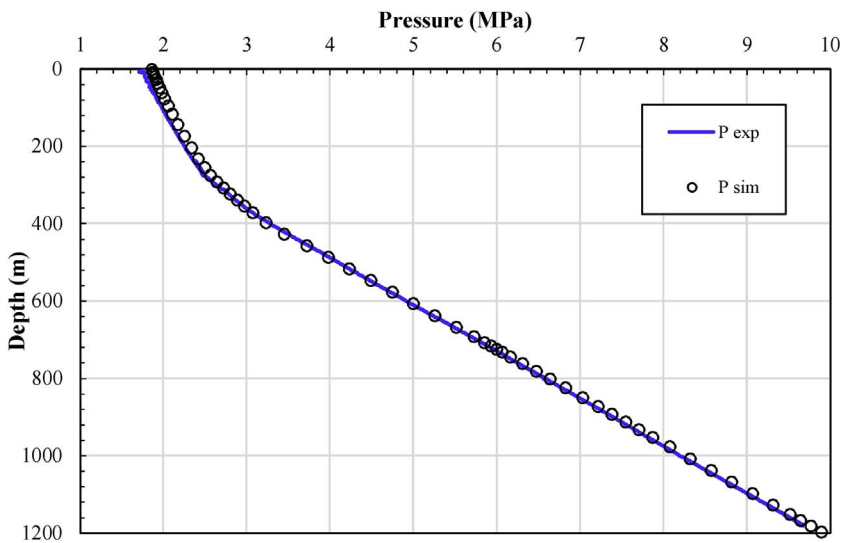


Fig. 11. Comparison between measured and simulated flowing pressure. The two set of data show a fairly good agreement, with major differences in correspondence of feed inflows, at the flash depth, and in the upper well section above FEED1.

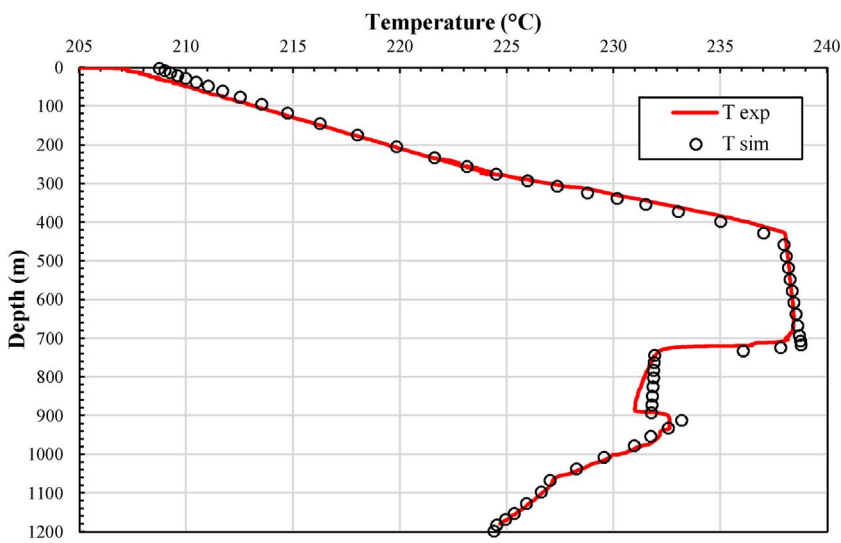


Fig. 12. Comparison between measured and simulated flowing temperature. The two sets of data show a good agreement, apart for the upper well section.

the vigorous airflow which was sucked into the separator inlet pipe through holes drilled in the inlet pipe plate. The air increases the gas phase velocity in the vertical separator pipe, thereby reducing

separation efficiency. High critical pressure (absolute pressure) at the lip pipe (up to 0.9 MPa), higher than the upper limit of 0.44 MPa for which the method was calibrated in the field (James, 1962), was

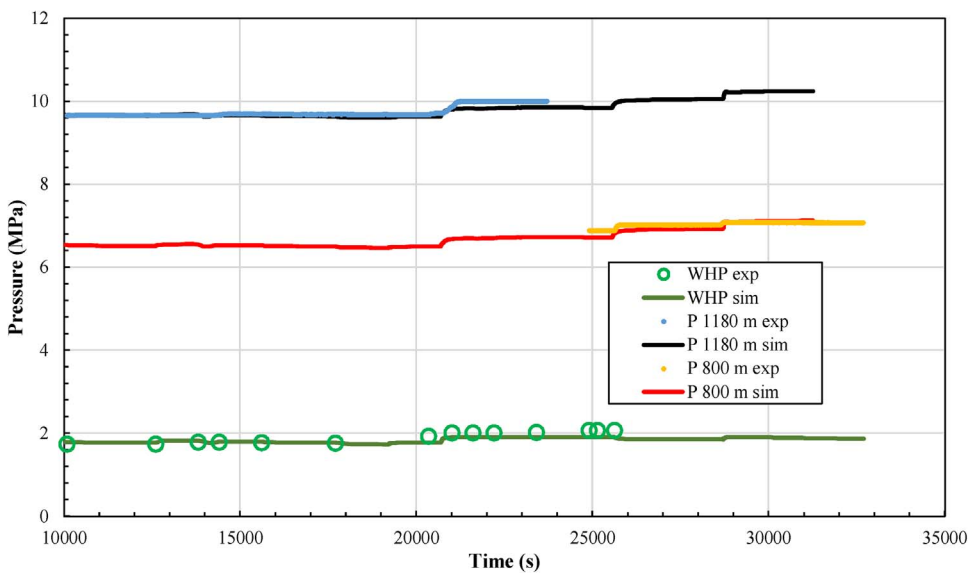


Fig. 13. Flowing downhole pressure and WHP: simulated results compared with field measurements.

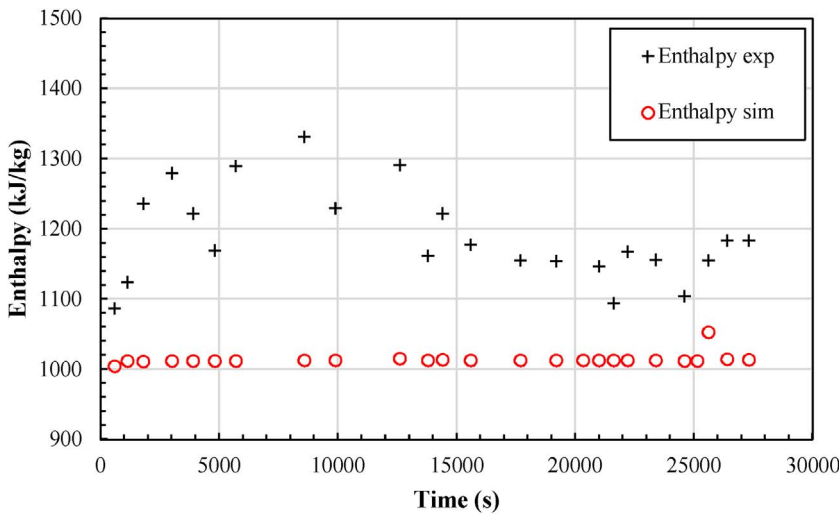


Fig. 14. Measured and simulated wellhead production enthalpy.

used. To this regard, it should be remembered that a theoretical assessment of James' method performed by Karamarakar and Cheng (1980) showed that up to lip pressures of 1.03 MPa the method shows the same deviation between empirical and theory results. The calculation of mass rate and enthalpy should also take NaCl and CO<sub>2</sub> content into account. Even if the CO<sub>2</sub> content is not huge, at the highest lip pressures recorded (from 0.24 to 0.9 MPa), the dryness fraction is low and CO<sub>2</sub> partial pressure represents a remarkable fraction of measured lip pressure.

Fig. 15 shows the comparison between the measured and simulated output curves. While measured WHP is well reproduced at rates above 20 kg s<sup>-1</sup>, at lower rates the simulated WHP underestimates the measured values.

As maximum discharge pressure is closely related to the production enthalpy, this may suggest that production enthalpy could actually be higher than that simulated. It follows that the inflow of higher enthalpy fluid from the upper feed (FEED1), not considered in this preliminary study should be further investigated.

6. Conclusion

T2Well, a coupled wellbore-reservoir numerical simulator was applied to improve outcomes of simulations of well tests in geothermal reservoirs, integrating downhole and surface measurements. T2Well,

coupled to the EWASG EOS module of TOUGH V.2.0, was able to model the thermodynamics and compute the phase properties of 3-component H<sub>2</sub>O-NaCl-CO<sub>2</sub> geothermal mixtures at typical conditions found in currently exploited high enthalpy geothermal reservoirs. T2Well-EWASG was verified, on the basis of a new time function included to model wellbore heat transfer using the Ramey (1962) analytical approach, and validated by simulating flowing P & T logs reported in the literature, and by simulating a short-duration production test performed on a high enthalpy geothermal well. This latter application of the coupled wellbore-reservoir simulator applied to the WW-01 slim hole drilled in the Wotten Waven Field (Commonwealth of Dominica), demonstrates that T2Well-EWASG can successfully be used as a tool to improve the integrated interpretation of surface and downhole measurements collected by production tests in geothermal wells. Simulations considering two major feeds but not a shallower inferred feed suggest a possible higher enthalpy contribution from the upper feed at rates lower than 20 kg s<sup>-1</sup>. Future work on WW-01 should aim to model the contribution of the first feedzone with a view to achieving a better match of discharge enthalpy and WHP at low rates. Inverse simulation techniques would be an important step forward, improving reproduction of field measurements with coupled wellbore-reservoir flow simulations. This would allow inclusion of a wider range of reservoir thermodynamic conditions and reservoir formation fluid composition and hydraulic properties, thereby improving matching with observed surface and downhole parameters. To this end, we consider it

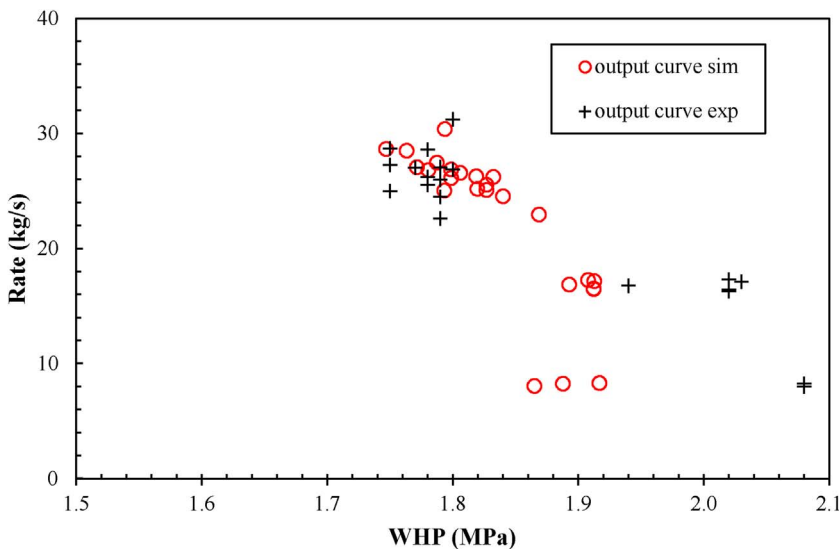


Fig. 15. Output curve: comparison between simulated results and measured data.

will be necessary to apply automatic inverse techniques. Options considered involve the use of PEST (Doherty, 2005), the integration of T2Well into iTOUGH2 (Finsterle, 2007) or the use of iTOUGH2 implementing the PEST protocol (Finsterle, 2011).

Our study enhanced the analytical computation of heat exchange between wellbore and formation by extending its validity to the initial production period and introducing the overall heat transfer coefficient, which allows the thermal resistivity of the wellbore completion to be taken into account. Developed for constant wellbore temperatures, the analytical solution we implemented could be improved by applying the principle of superposition of effects according to Zhang et al., 2011.

## Acknowledgements

The Authors thank the Geothermal Project Management Unit (PMU) of the Commonwealth of Dominica and ELC Electroconsult SpA for permission to use well WW-01 field data. This study was in part supported by Saipem SpA within the framework of the R & D Project “Simulation of production tests with TOUGH2-T2Well”.

## References

- Axelsson, G., 2013. Geothermal well testing. Presented at Short Course V on Conceptual Modelling of Geothermal Systems, organized by UNU-GTP and LaGeo, in Santa Tecla, El Salvador, February 24–March 2, 2013.
- Barelli, A., Corsi, R., Del Pizzo, G., Scali, C., 1982. A two-phase flow model for geothermal wells in the presence of non-condensable gas. *Geothermics* 11 (3), 175–191.
- Battistelli, A., Calore, C., Pruess, K., 1997. The simulator TOUGH2/EWASG for modelling geothermal reservoirs with brines and a non-condensable gas. *Geothermics* 26 (4), 437–464.
- Battistelli, A., 2008. Modeling multiphase organic spills in coastal sites with TMVOC V.2.0. *Vadose Zone J.* 7, 316–324.
- Battistelli, A., Marcolini, M., 2009. TMGAS: a new TOUGH2 EOS module for the numerical simulation of gas mixtures injection in geological structures. *Intl. J. Greenhouse Gas Control* 3, 481–493.
- Battistelli, A., 2012. Improving the Treatment of Saline Brines in EWASG for the Simulation of Hydrothermal Systems. In: *Proceedings of TOUGH Symposium*. Lawrence Berkeley National Laboratory Berkeley, California, pp. 17–19 September.
- Bhat, A., Swenson, D., Gosavi, S., 2005. Coupling the HOLA wellbore simulator with TOUGH2. In: *Proceedings of the 30th Workshop on Geothermal Reservoir Engineering Stanford University*. Stanford, California, USA.
- Björnsson, G., 1987. A Multi-feedzone Geothermal Wellbore Simulator. University of California, USA Berkeley.
- Bonduá, S., Berry, P., Bortolotti, V., Cormio, C., 2012. TOUGH2Viewer: a post-processing tool for interactive 3D visualization of locally refined unstructured grids for TOUGH2. *Comp. Geosci.* 46, 107–118.
- Bonduá, S., Battistelli, A., Berry, P., Bortolotti, V., Consonni, A., Cormio, C., Geloni, C., Vasini, E.M., 2015. 3D Voronoi pre- and post-processing tools for the modeling of deep sedimentary formations with the TOUGH2 family of codes. In: *Proceedings, TOUGH Symposium 2015*. Lawrence Berkeley National Laboratory, Berkeley, California. pp. 28–30 September.
- Bonduá, S., Battistelli, A., Berry, P., Bortolotti, V., Consonni, A., Cormio, C., Geloni, C., Vasini, E.M., 2016. 3D Voronoi grid dedicated software for modeling gas migration in deep layered sedimentary formations with TOUGH2-TMGAS. *Comp. Geosci.* Corrected Proof. <http://dx.doi.org/10.1016/j.cageo.2017.03.008>. in press.
- H.C. Carslaw, J.C. Jaeger. 1959 *Conduction of Heat in Solids*, second edition Oxford University Press
- Chiu, K., Thakur, S.C., 1959. 1991. Modeling of wellbore heat losses in directional wells under changing injection conditions. SPE 22870. In: *Presented at SPE Annual Technical Conference and Exhibition*. October, 1991, Dallas, Texas. pp. 517–528.
- Croucher, A.E., O’Sullivan, M.J., 2008. Application of the computer code TOUGH2 to the simulation of supercritical conditions in geothermal systems. *Geothermics* 37, 622–634.
- Doherty, J., 2005. *Watermark Numerical Computing*. PEST, Model-independent Parameter Estimation, 5th edition. User Manual.
- Driesner, T., Heinrich, C.H., 2007. The system H<sub>2</sub>O–NaCl. Part I: correlation formulae for phase relations in temperature–pressure–composition space from 0 to 1000 °C, 0 to 5000 bar, and 0 to 1 XNaCl. *Geochem. Cosm. Acta* 71, 4880–4901.
- Driesner, T., 2007. The system H<sub>2</sub>O–NaCl, part II: correlations for molar volume, enthalpy, and isobaric heat capacity from 0 to 1000 °C, 1 to 5000 bar, and 0 to 1 XNaCl. *Geochem. Cosm. Acta* 71, 4902–4919.
- Electroconsult, E.L.C., 2013. 2013. Wotten Waven geothermal field, Commonwealth of Dominica, West Indies: feasibility study. Report for the Ministry of Public Utilities. Energy and Ports, Commonwealth of Dominica (unpublished).
- Finsterle, S., Sonnenthal, E.L., Spycher, N., 2014. Advance in subsurface modeling using the TOUGH suite of simulators. *Comp. Geosci.* 65, 2–12.
- Finsterle, S., 2007. *iTOUGH User’s Guide*, Earth Science Division. Lawrence Berkeley National Laboratory, University of California, Berkeley, CA 94720.
- Finsterle, S., 2011. *iTOUGH2 Universal Optimization Using the PEST Protocol*. User’s Guide. Earth Science Division, Lawrence Berkeley National Laboratory, University of California, Berkeley, CA 94720, Report LBNL–3698E.
- Gudmundsdottir, H., Jonsson, M.T., 2015. The wellbore simulator flowell—model enhancement and verification. In: *Proceedings World Geothermal Congress 2015*. Melbourne, Australia, April 19–25.
- Gudmundsdottir, H., Jonsson, M.T., Palsson, H., 2012. A coupled wellbore-reservoir simulator utilizing measured wellhead conditions. In: *Proceedings 53rd SIMS Conference on Simulation and Modeling*. The National Energy Authority (NEA), Reykjavik October 3–6.
- Hagdu, T., Zimmerman, R., Bodvarsson, G., 1995. Coupled Reservoir-Wellbore Simulation of Geothermal. *Reservoir Behavior Geothermics* 24 (2), 145–166.
- International Association for the Properties of Water and Steam, 1997. *Release on the IAPWS Industrial Formulation 1997 for the Thermodynamic Properties of Water and Steam*. Erlangen, Germany.
- International Association for the Properties of Water and Steam, 2008. *Release on the IAPWS Formulation 2008 for the Viscosity of Ordinary Water Substance*. Berlin, Germany.
- James, C.R., 1962. Steam-water critical flow through pipes. *Proc. Institute of Mech. Eng.* 176 (26), 741.
- James, R., 1975. Gas content of a hot-water reservoir estimated from downhole pressure and temperature measurements. In: *Berkeley, CA. Second United Nations Symposium* 3. pp. 1689–1691.
- Karamarakar, M., Cheng, P., 1980. A theoretical assessment of James’ method for the determination of geothermal wellbore discharge characteristics. *Geoth. Res. Eng. Manag. Program*, report LBL- 11498, GREMP-12, UC-66a.
- Oldenburg, C.M., Pan, L., 2013. Porous media compressed-air energy storage (PM-CAES): theory and simulation of the coupled wellbore reservoir system. *Transp. Porous Media* 97 (2), 201–221.
- Oldenburg, C.M., Freifeld, B.M., Pruess, K., Pan, L., Finsterle, S., Moridis, G.J., 2011. Numerical simulations of the Macondo well blowout reveal strong control of oil flow by reservoir permeability and exsolution of gas. In: *In: Marcia McNutt, K. (Ed.), Proc. Of the National Academy of Sciences of the United States of America* 109. pp. 20254–20259.
- Osborn, W., Hernández, J., George, A., 2014. Successful Discovery Drilling in Roseau Valley, Commonwealth of Dominica. *Proc., 39th Workshop on Geothermal Reservoir Engineering Stanford U., Stanford, CA, February 24–26, SGP-TR-202*.
- Pan, L., Oldenburg, C.M., 2013. T2Well—an integrated wellbore-reservoir simulator. *Comp. Geosci.* 65, 46–55.
- Pan, L., Oldenburg, C.M., Wu, Y., Pruess, K., 2011. T2Well/ECO2N Version 1.0: Multiphase and Non-Isothermal Model for Coupled Wellbore-Reservoir Flow of Carbon Dioxide and Variable Salinity Water. Earth Sciences Division, Lawrence Berkeley National Laboratory, University of California, Berkeley, California 94720.
- Pan, L., Freifeld, B., Doughty, C., Zakem, S., Sheu, M., Cutright, B., Terrail, T., 2015. Fully coupled wellbore-reservoir modelling of geothermal heat extraction using CO<sub>2</sub> as the working fluid. *Geothermics* 53, 100–113.
- Pruess, K., 2005. EGN: A TOUGH2 Fluid Property Module for Mixtures of Water, NaCl, and CO<sub>2</sub>, Report LBNL -57952. Lawrence Berkeley National Laboratory, Berkeley Calif 02.
- Pruess, Oldenburg, C., Moridis, G., 1999. *Tough User’s Guide, Version 2.0*, Earth Sciences Division, Lawrence Berkeley National Laboratory. University of California Berkeley Calif. h2.
- Ramey, H.J., 1962. *Wellbore Heat Transmission*. Mobil Oil Co. Santa Fe Springs, California.
- Shi, H., Holmes, J.A., Durlifsky, L.J., Aziz, K., Diaz, L.R., Alkaya, B., Oddie, G., 2005. Drift-flux modeling of two-phase flow in wellbores. *Soc. Pet. Eng. J.* 10 (1), 24–33.
- Tokita, H.H., Lima, E., Hashimoto, K., 2005. A Middle-Term Power Output Prediction at the Hatchobaru Field by Coupling Multifeed Wellbore Simulator and Fluid-Gathering Pipeline Simulator to Reservoir Simulator. In: *Proceedings of World Geothermal Congress Antalya, Turkey*, pp. 24–29 April.
- Tokita, H., Itoi, R., 2004. Development of the MULFEWS multi-feed wellbore simulator. *Proceedings of the 29th Workshop on Geothermal. Reservoir Engineering Stanford University Stanford, California, USA*.
- Zhang, K., Wu, Y.-S., Pruess, K., 2008. *User’s Guide for TOUGH2-MP—A Massively Parallel Version of the TOUGH2 Code*, Report LBNL-315E. Lawrence Berkeley National Laboratory, Berkeley, Calif.
- Zhang, Y., Pan, L., Pruess, K., Finsterle, S., 2011. A time-convolution approach for modeling heat exchange between a wellbore and surrounding formation. *Geothermics* 40 (4), 261–266.
- Zuber, N., Findlay, J.A., 1965. Average volumetric concentration in two-phase flow systems. *J. Heat Transfer* 87, 453.